Inorganic Chemistry

Communication

pubs.acs.org/IC

ABX_3-Type Organic–Inorganic Hybrid Phase Transition Material: 1-Pentyl-3-methylimidazolium Tribromoplumbate

Tianliang Chen, Yuelan Zhou, Zhihua Sun, Shuquan Zhang, Sangen Zhao, Yuanyuan Tang, Chengmin Ji, and Junhua Luo*

Key Laboratory of Optoelectronic Materials Chemistry and Physics, Fujian Institute of Research on the Structure of Matter, Chinese Academy of Sciences, Fuzhou, Fujian 350002, China

Supporting Information

ABSTRACT: A new one-dimensional ABX_3-type organic–inorganic hybrid phase transition compound, 1-pentyl-3-methylimidazolium tribromoplumbate (**1**), where the Pb^{II} ion exhibits hemicoordination geometry, resulting in anionic $(PbBr_3)_n$ chains of an edge-shared $PbBr_5$ polyhedron, has been successfully synthesized. **1** undergoes a reversible second-order phase transition at about 136 K. The dielectric constants of **1** exhibit an obvious steplike anomaly tuned between a high dielectric state in the high-temperature phase and a low state in the low-temperature phase. The origin of its phase transition is ascribed to the order–disorder transformation of the cation coupled with the relative displacement of the Br atoms. These findings provide a new approach to exploring a novel ABX_3-type compound with functional phase transition properties.

Solid–solid structural phase transition materials, considered as an effective strategy for the design of functional materials such as ferroelectric materials, nonlinear-optical switches, and switchable dielectric devices,[1−3] have been attracting great interest in the past decades because of the prospect of applications in the field of data storage, signal processing, environmental monitoring, etc.[4] Among them, ABX_3-type hybrid organic–metal halide (OMH) phase transition materials have been paid special attention because of the possibility for their use in constructing perovskite materials, which have recently (within the last 5 years) been considered as the most competitive candidates for solar cells, such as $CH_3NH_3PbX_3$ (X = Cl, Br I).[5] In this case, considerable effort has recently been devoted to the development of ABX_3-type hybrid structures as phase transition materials.[6] For instance, Ye et al. used a 3-pyrroline heterocycle as the artificial molecular motor to construct a new ABX_3-type hybrid OMH ferroelectric [(3-pyrrolinium)$(CdCl_3)$], where the 3-pyrrolinium ring presents a swinglike motion around the N atom.[6f] As the characteristic divalent ion with lone-pair electrons, the Pb^{II} ion makes the construction of ABX_3-type hybrid OMH compounds easier.[7] Furthermore, there are even some Pb-based OMH compounds with the classical ABX_3-type perovskite structure.[8] However, Pb-based ABX_3-type OMH compounds with structural phase transition are still very sparse to date.[8c,9]

Imidazole as a simple organic heterocyclic cation has been identified as a rotatory unit to develop functional phase materials such as switchable molecular dielectrics and ferroelectric materials.[10,11] Furthermore, it will afford a higher possibility of phase transition if the flexible alkyl chain is attached to the imidazole ring. In this work, we discovered a new ABX_3-type hybrid phase transition compound, 1-pentyl-3-methylimidazolium tribromoplumbate (**1**). Herein, we report its crystal structure and the investigation of its phase transition properties by single-crystal structure analyses, differential scanning calorimetry (DSC), and dielectric measurements.

Compound **1** was demonstrated to undergo structural phase transition by DSC measurements. As shown in Figure 1a, the

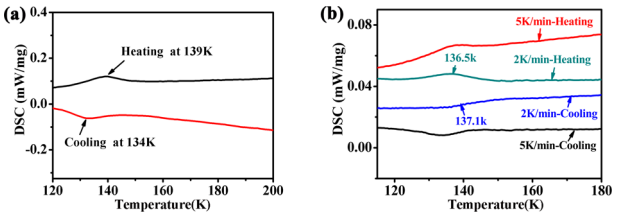

Figure 1. DSC curves (a) of **1** and (b) with different scanning rates for **1**.

DSC curves show two peaks at 134 and 139 K in cooling and heating runs, respectively, suggesting a reversible structural phase transition. The narrow thermal hysteresis, confirmed by DSC measurements with different scanning rates, indicates a characteristic of a second-order transition (Figure 1b).[12] The entropy change ΔS is 2.29 J/mol/K.

According to the Boltzmann equation ($\Delta S = R \ln N$), in which R is the gas constant and N is the ratio of the number of respective geometrically distinguishable orientations, N is equal to 1.89, showing a typical order–disorder feature.[13]

The crystal structures of **1** at 190 K (high-temperature phase, HTP) and 100 K (low-temperature phase, LTP) both crystallize in the space group of $P2_1/n$ (Table S1 in the Supporting Information, SI). The unit cell parameter anomalies as a function of the temperature can be further used as direct evidence to ascertain its second phase transition feature (Figure S2 in the SI). The asymmetric unit of **1** in both the HTP and LTP contains a crystallographically distinct Pb^{2+} cation, one 1-pentyl-3-methylimidazolium ($PMIm^+$) cation, and three Br^- anions, as shown in Figure 2. In the HTP, each Pb ion is hemidirected and five-coordinated by Br^- anions. Four Br^- anions link each Pb ion with two other Pb ions by μ_2-bridging connections, resulting in a

Received: April 19, 2015
Published: July 13, 2015

ACS Publications © 2015 American Chemical Society

DOI: 10.1021/acs.inorgchem.5b00891
Inorg. Chem. 2015, 54, 7136−7138

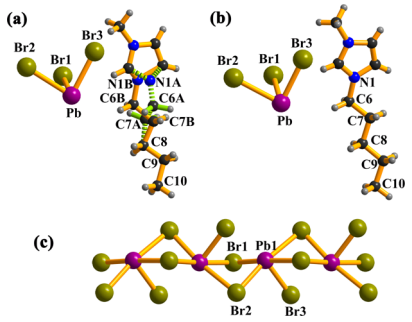

Figure 2. Asymmetric unit of **1** at (a) 190 K and (b) 100 K, respectively. (c) An infinite one dimensional Pb−Br−Pb chain of **1** at 190 K.

[$PbBr_5$] polyhedron and forming a one-dimensional zigzag chain along the [010] direction, as presented in Figures 2 and S3 in the SI. In particular, it must be emphasized that complex **1** is the first ABX_3 hybrid phase transition example with the five-coordinated geometry of the [$PbBr_5$] polyhedron, which is different from other reported ABX_3 hybrid phase transition compounds with the six-coordinated geometry of the MX_6 (M = divalent metal; X = halide ion) octahedron[6,8b,10]

With the temperature decreasing from the HTP to LTP, the bond lengths of Pb−Br are strikingly different. As shown in Figure 3a,b, the bond lengths of Pb−Br1 (3.16 Å) and Pb1−Br2

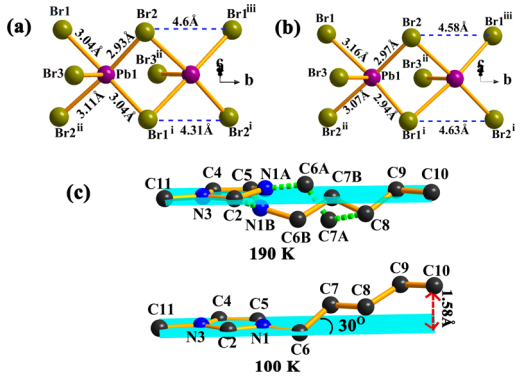

Figure 3. Pb−Br bond lengths and Br−Pb−Br angles of the $[PbBr_3]_n$ chain of **1** at (a) 190 K and (b) 100 K. (c) Configurations of the PMIm cation at 190 and 100 K. Atoms labeled with superscripts i−iii are at $(^3/_2 - x, {}^1/_2 + y, {}^1/_2 - z)$, $(^3/_2 - x, -{}^1/_2 + y, {}^1/_2 - z)$, and $(x, y + 1, z)$, respectively.

(2.97 Å) in the LTP are larger than the values of 3.04 and 2.93(0) Å in the HTP, while the bond lengths of Pb1−$Br1^i$ (2.94 Å) and Pb1−$Br2^{ii}$ (3.07 Å) in the LTP are shorter than the corresponding values of 3.04 and 3.11 Å in the HTP. These changes of the bond lengths of Pb−Br indicate that the Br1 and Br2 atoms are displaced in the opposite direction along the *b* axis. Such relative displacement of the Br atom can be further deduced from the change of the distances of the adjacent two Br atoms. As shown in Figure 3a,b, the distances of $Br1^i$···$Br2^i$ and $Br1^{iii}$···Br2 in the HTP are 4.34 and 4.6 Å, while the values have been changed to 4.63 and 4.58 Å in the LTP, respectively. These facts suggest that the Br1 and Br2 atoms undergo a reverse shift along the *b* axis during the phase transition process.

Besides, for the cationic part, it shows marked differences in their configuration at the LTP. At the HTP, it is evident to note that both the imidazole ring and pentyl of the $PMIm^+$ cation are partially disordered. Such distinct disorder characteristics can be directly revealed by the large anomalous elongations of thermal ellipsoids of the C and N atoms (Figure S4 in the SI). With the temperature decreasing from the HTP to LTP, the $PMIm^+$ cation is frozen (Figure 2b) and the alkyl chain can give rise to the deviations of the relative atomic positions in the cationic part. As illustrated in Figure 3c, in the HTP, all of the atoms in the $PMIm^+$ cation almost lie in plane 1 determined by C11, N3, C4, and C2, while in the LTP, the atoms C7, C8, C9, and C10 are significantly deviated from plane 1. The dihedral angle between plane 1 and the plane determined by the atoms C7, C8, C9, and C10 is 30°, and the largest deviation value for the C10 atom is 1.58 Å. Therefore, it can be proposed that the order−disorder transformation of the partial cation coupled with the displacement of the Br atoms may be mainly responsible for the structural phase transition.

A pressed-powder pellet of **1** was used in dielectric measurements under different frequencies. Figure 4 displays

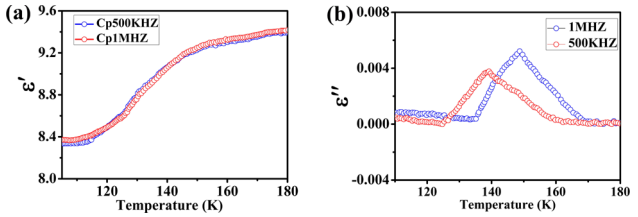

Figure 4. (a) Real (ε') and (b) imaginary (ε'') parts of the dielectric permittivity at frequencies of 500 kHz and 1 MHz.

the real (ε') and imaginary (ε'') parts of the dielectric permittivity of **1**. In the heating mode, the dielectric constants remain low stable values until the temperature reaches 130 K, exhibit a distinct increase with a clear slope, and then remain a high constant, indicating the occurrence of the phase transition. The dielectric loss shows temperature dependence, with a broad peak approaching T_c during the heating process (Figure 4b). What interests us is the existence of two plateaus of the permittivity, which is consistent with the characteristic of switchable molecular dielectrics.[1]

In summary, an ABX_3-type organic−inorganic hybrid phase transition compound (**1**), where the Pb^{II} ion exhibits hemi-coordination geometry, has been synthesized. **1** undergoes a solid-state second-order phase transition around 136 K. Furthermore, its dielectric constants can be switched between a high dielectric state in the HTP and a low state in the LTP. The origin of its phase transition is triggered by the order−disorder transformation of the cation coupled with the relative displacement of the Br atoms. We believe that the present findings provide a new avenue for building ABX_3-type organic−inorganic compounds with functional phase transition.

■ ASSOCIATED CONTENT

Supporting Information

Experimental details and characterizations of **1** and X-ray crystallographic data in CIF format (CCDC 1022535 and 1022536). The Supporting Information is available free of charge on the ACS Publications website at DOI: 10.1021/acs.inorgchem.5b00891.

■ AUTHOR INFORMATION

Corresponding Author

*E-mail: jhluo@fjirsm.ac.cn.

DOI: 10.1021/acs.inorgchem.5b00891
Inorg. Chem. 2015, 54, 7136−7138

Notes

The authors declare no competing financial interest.

■ ACKNOWLEDGMENTS

This work was supported by the NSFC (Grants 21222102, 21373220, 51402296, 21171166, and 21301172), the 973 Key Program of MOST (Grant 2011CB935904), and the NSF for Distinguished Young Scholars of Fujian Province (Grant 2014J06015).

■ REFERENCES

(1) (a) Zhang, W.; Ye, H.-Y.; Graf, R.; Spiess, H. W.; Yao, Y.-F.; Zhu, R.- Q.; Xiong, R.-G. *J. Am. Chem. Soc.* **2013**, *135*, 5230−5233. (b) Sun, Z. H.; Wang, X. Q.; Luo, J. H.; Zhang, S. Q.; Yuan, D. Q.; Hong, M. C. *J. Mater. Chem. C* **2013**, *1*, 2561−2567. (c) Sun, Z. H.; Luo, J. H.; Chen, T. L.; Li, L. N.; Xiong, R.-G.; Tong, M.-L.; Hong, M. C. *Adv. Funct. Mater.* **2012**, *22*, 4855−4861.

(2) (a) Sun, Z. H.; Luo, J. H.; Zhang, S. Q.; Ji, C. M.; Zhou, L.; Li, S. H.; Deng, F.; Hong, M. C. *Adv. Mater.* **2013**, *25*, 4159−4163. (b) Bi, W.; Louvain, N.; Mercier, N.; Luc, J.; Rau, I.; Kajzar, F.; Sahraoui, B. *Adv. Mater.* **2008**, *20*, 1013−1017. (c) Fu, D.-W.; Zhang, W.; Cai, H.-L.; Ge, J.-Z.; Zhang, Y.; Xiong, R.-G. *Adv. Mater.* **2011**, *23*, 5658−5662.

(3) (a) Zhang, Y.; Zhang, W.; Li, S.-H.; Ye, Q.; Cai, H.-L.; Deng, F.; Xiong, R.-G.; Huang, S. D. *J. Am. Chem. Soc.* **2012**, *134*, 11044−11049. (b) Ye, H.-Y.; Zhang, Y.; Noro, S.; Kubo, K.; Yoshitake, M.; Liu, Z.-Q.; Cai, H.-L.; Fu, D.-W.; Yoshikawa, H.; Awaga, K.; Xiong, R.-G.; Nakamura, T. *Sci. Rep.* **2013**, *3*, 2650 DOI: 10.1038/srep02650. (c) Zhang, Y.; Ye, H.-Y.; Fu, D.-W.; Xiong, R.-G. *Angew. Chem.* **2014**, *126*, 2146−2150. (d) Horiuchi, S.; Kumai, R.; Tokura, Y. *J. Am. Chem. Soc.* **2013**, *135*, 4492−4500. (e) Fu, D.-W.; Cai, H.-L.; Liu, Y. M.; Ye, Q.; Zhang, W.; Zhang, Y.; Chen, X.-Y.; Giovannetti, G.; Capone, M.; Li, J. Y.; Xiong, R.-G. *Science* **2013**, *339*, 425−428.

(4) (a) Yu, Y.; Nakano, M.; Ikeda, T. *Nature* **2003**, *425*, 145. (b) Wuttig, M.; Yamada, N. *Nat. Mater.* **2007**, *6*, 824−832. (b) Samoc, M.; Gauthier, N.; Cifuentes, M. P.; Paul, F.; Lapinte, C.; Humphrey, M. G. *Angew. Chem., Int. Ed.* **2006**, *45*, 7376−7379.

(5) (a) Lee, M. M.; Teuscher, J.; Miyasaka, T.; Murakami, T. N.; Snaith, H. J. *Science* **2012**, *338*, 643−647. (b) Norris, D. J.; Aydil, E. S. *Science* **2012**, *338*, 625−626. (c) Liu, M. Z.; Johnston, M. B.; Snaith, H. J. *Nature* **2013**, *501*, 395−398.

(6) (a) Zhang, Y.; Ye, H.-Y.; Zhang, W.; Xiong, R.-G. *Inorg. Chem. Front.* **2014**, *1*, 118−123. (b) Zhang, Y.; Liao, W.-Qiang.; Fu, D.-W.; Ye, H.-Y.; Chen, Z.-N.; Xiong, R.-G. *J. Am. Chem. Soc.* **2015**, *137*, 4928−4931. (c) Qin, L.-L.; Ye, H.-Y.; Wang, D.-Y. *Inorg. Chem. Commun.* **2014**, *46*, 47−50. (d) Liao, W.-Q.; Ye, H.-Y.; Zhang, Y.; Xiong, R.-G. *Dalton Trans.* **2015**, *44*, 10614. (e) Jin, J.; Jin, L.; Su, E.-B. *CrystEngComm* **2014**, *16*, 9284−9290. (f) Ye, H.-Y.; Zhang, Y.; Fu, D.-W.; Xiong, R.-G. *Angew. Chem.* **2014**, *126*, 11424−11429.

(7) (a) Coleman, F.; Feng, Guo.; Murphy, R. W.; Nockemann, P.; Seddon, K. R.; Swadźba-Kwaśny, M. *DaltonTrans* **2013**, *42*, 5025−5035. (b) Billing, D. G.; Lemmerer, A. *CrystEngComm* **2006**, *8*, 686−695. (c) Li, Y.; Lin, C.; Zheng, G.; Lin, J. *J. Solid State Chem.* **2007**, *180*, 173−179.

(8) (a) Stoumpos, C. C.; Malliakas, C. D.; Kanatzidis, M. G. *Inorg. Chem.* **2013**, *52*, 9019−9038. (b) Dang, Y.; Liu, Y.; Sun, Y.; Yuan, D.; Liu, X.; Lu, W.; Liu, G.; Xia, H.; Tao, X. *CrystEngComm* **2015**, *17*, 665−670. (c) Baikie, T.; Fang, Y.; Kadro, J. M.; Schreyer, M.; Wei, F.; Mhaisalkar, S. G.; Graetzel, M.; White, T. J. *J. Mater. Chem. A* **2013**, *1*, 5628−5641.

(9) (a) Vaněk, P.; Havránková, M.; Hybler. *Solid State Commun.* **1992**, *82*, 509−512. (b) Swainson, I. P.; Hammond, R. P.; Soullière, C.; Knop, O.; Massa, W. *J. Solid State Chem.* **2003**, *176*, 97−104.

(10) (a) Piecha, A.; Białońska, A.; Jakubas, R. *J. Mater. Chem.* **2012**, *22*, 333−336. (b) Pajãk, Z.; Czarnecki, P.; Szafrańska, B.; Małuszyńska, H.; Fojud, Z. *J. Chem. Phys.* **2006**, *124*, 144502. (c) Pajak, Z.; Czarnecki, P.; Szafrańska, B.; Małuszyńska, H.; Fojud, Z. *Phys. Rev. B: Condens. Matter Mater. Phys.* **2004**, *69*, 132102.

(11) (a) Fukumoto, T.; Kashida, S. *J. Phys. Soc. Jpn.* **1985**, *54*, 3785−3795. (b) Heyns, A. M.; Schutte, C. J. H. *J. Mol. Struct.* **1971**, *8*, 339−349. (c) Tornero, J. D.; Cano, F. H.; Payos, J.; Martinez-Ripoll, M. *Ferroelectrics* **1978**, *19*, 123−130. (d) Gesi, K. *J. Phys. Soc. Jpn.* **1990**, *59*, 432−434.

(12) Fu, D. W.; Zhang, W.; Cai, H. L.; Zhang, Y.; Ge, J. Z.; Xiong, R. G.; Huang, S. D.; Nakamura, T. *Angew. Chem.* **2011**, *123*, 12153−12157.

(13) (a) Jain, P.; Ramachandran, V.; Clark, R. J.; Zhou, H. D.; Toby, R. H.; Dalal, N. S.; Kroto, H.; Cheetham, A. K. *J. Am. Chem. Soc.* **2009**, *131*, 13625−13627. (b) Fu, D.-W.; Cai, H.-L.; Li, S. H.; Ye, Q.; Zhou, L.; Zhang, W.; Zhang, Y.; Deng, F.; Xiong, R. G. *Phys. Rev. Lett.* **2013**, *110*, 257601−257605.

DOI: 10.1021/acs.inorgchem.5b00891
Inorg. Chem. 2015, 54, 7136−7138